Final Report

Reduction of wing-tip vortex through wing design

Group 11-04

Lau Tat Hong 4O3 Chua Bing Heng 4O3 Isaac Tan Jia Le 3P3

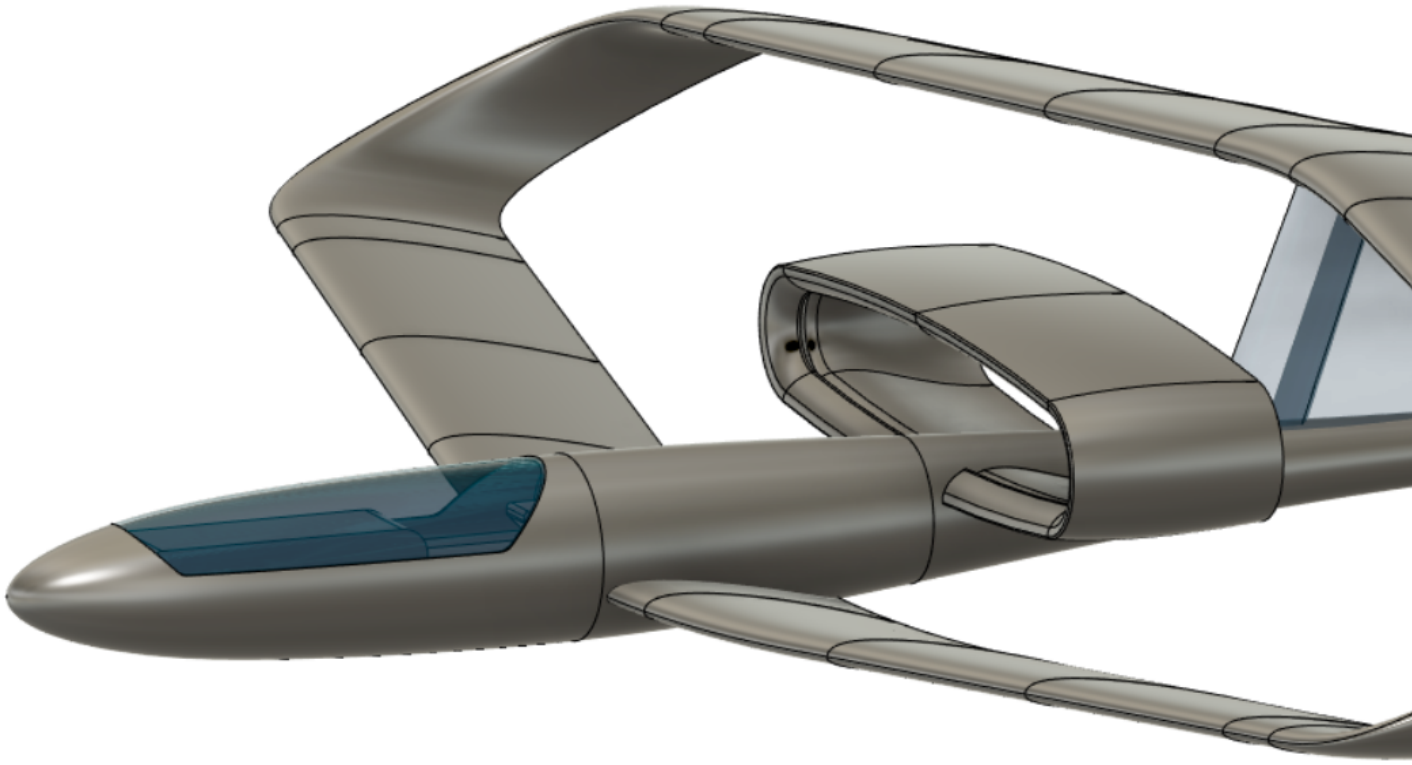

~ Inspired by Sir James Dyson, British inventor, founder and CEO of Dyson.

Abstract

For many years, consumer airplanes have kept the same rough design of its wings and engine, leading to inefficient use of fuel. By tapping into newer, more efficient designs, one can reduce the fuel consumption and fuel cost per flight greatly worldwide. This project investigates the feasibility of reducing the effect of the wing-tip vortex phenomenon, while also attempting to increase the efficiency of a standard propulsion system through preserving flow linearity. This will be done through a prototype plane - *Avis* - which is a model of a much more fuel-efficient design. The design features a box-wing design, which aims to reduce the effect of wingtip vortices and thus reduce induced drag, creating greater fuel efficiency; along with a new propulsion system that preserves flow linearity, multiplies the effect of a propeller in moving the plane. The *Avis* is remotely controlled with the help of a standard flight controller, making it easy to reproduce with any other controller. 3D models, physical prototypes and computational fluid dynamics were used in determining the structural integrity of the *Avis* and its aerodynamics. The usage of computer-aided design helps to ensure that the proposed solution is one that is feasible and workable, without having to waste excessive material. This paper concludes that the proposed solutions can be effective in reducing induced drag in commercial airliners, which ultimately leads to lower energy consumption.

Contents

Introduction

Since the start of time, humans have let their curiosity draw them to the skies. Insects were the first of all animals to evolve flight, and have set the dominoes in motion for humans to explore the world above ground.

Ever since the Wright brothers built the world's first successful motor-powered airplane, the aerospace industry has been rapidly innovating and evolving. In 2017, the aerospace industry was worth 838 billion USD. (Aboulafia, Michaels; 2018) The number goes to show how aerospace engineering has come a long way since 18th-century scientists began to understand fluid dynamics. Today, the aerospace industry has become a part of our lives. We take planes overseas on trips, our mail comes from overseas through airlifted cargo and fighter jets defend our borders.

However, the aerospace industry has reached a point where further optimisation of standard aircraft modules no longer brings breakthroughs in plane efficiency and safety. What humanity requires is a new model that solves present day issues on induced drag. Hence, our project seeks to experiment upon a redesigned propulsion and wing system capable of solving vortice induced drag issues through the preservation of flow linearity.

Rationale

Wingtip vortices

Induced drag, or parasitic drag, is an aerodynamic drag force that occurs whenever a moving object redirects the airflow coming at it. This drag force occurs in airplanes due to wings or a lifting body redirecting air to cause lift and redirecting air to cause a downforce, creating wingtip vortices. (Skybrary, 2020) Such parasitic drag reduces the energy efficiency of planes by wasting introduced energy upon the generation of vortices instead of the production of thrust, thereby wasting additional expense and limiting the capability of planes. Vortices also form wake turbulence trailing the plane, introducing a turbulent, hazardous airspaces that can cause major flight issues. (FAA, 2014)

Fig 4.1: Wingtip vortices in action (NASA)

Flow linearity

The second issue is flow linearity. When a propeller generates motion, there are multiple axes in which the motion is translated to, thus only a certain amount of that propulsion would be useful in moving the plane forwards, causing standard propellers to be inefficient in producing thrust. Therefore, a system that reduces this parasitic drag, and instead preserves the horizontal flow of air, would be crucial in maximising the efficiency of planes in this day and age.

Case study

On the 12th of November, 2001, American Airlines Flight 587 crashed into the neighbourhood of Belle Harbor, Queens, shortly after takeoff from John F. Kennedy International Airport, en route to Santo Domingo. When Flight 587 had climbed to 13,000 feet, it encountered the wake turbulence from the Japan Airlines flight before it. In response, the first officer of Flight 587 alternated between moving the rudder from right to left quickly. Eventually, the lateral force caused the vertical stabilizer to separate from the aircraft. Without the stabiliser, the aircraft pitched downwards, and went into a flat spin, as the pilots struggled to maintain control. The craft eventually crashed into Beach 131 Street, a residential area in queens. (Ranter, 2001)

Such tragedies can be prevented through design optimisation of aircraft, thereby our project objective; preserving the flow linearity of aircraft, hence eliminating vortex drag and maximising efficiency.

Design

Bernoulli’s principle

In fluid dynamics, Bernoulli's principle states that an increase in the speed of a fluid occurs simultaneously with a decrease in static pressure or a decrease in the fluid's potential energy. (Batchelor, 1967)

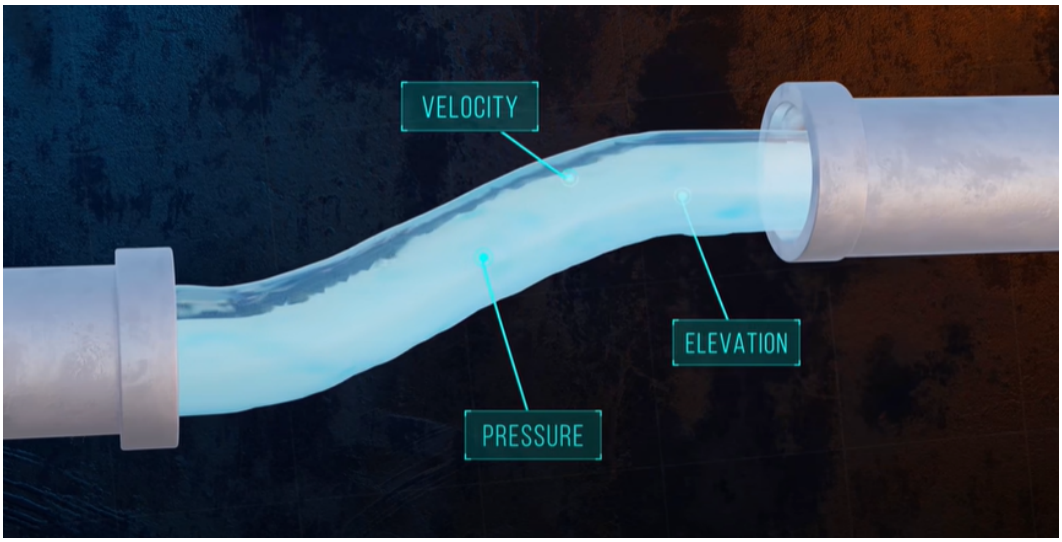

Fig 5.1: Visualisation of Bernoulli’s principle

Bernoulli’s principle is represented as such :

$$P_1 + \frac{1}{2}\rho v_1^{\,2} + \rho g h_1 = constant$$

where $P$is fluid pressure

ρ is fluid density

v is fluid velocity

g is gravitational acceleration

h is elevation

In other words, Static pressure + Fluid kinetic energy per unit volume + Pressure exerted by fluid due to gravity = constant

Wing system

Theory of flight

In order for an aircraft to achieve flight, a lift force that equals or exceeds the aircraft's weight must be applied. The fluid exerts a force on the airfoil as it moves through it, and this force can be split into the vertical and horizontal components, lift and drag respectively. (MIT, 1997)

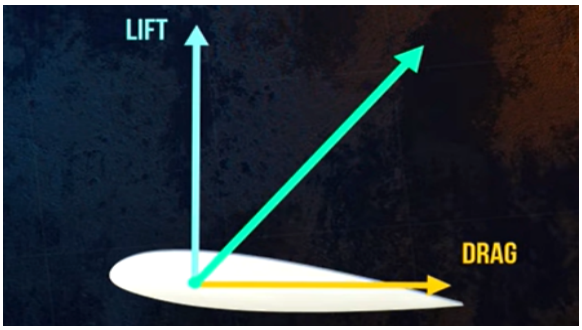

Fig 5.2: Components of lift

Lift can be represented as such:

$$L = c_l \cdot \frac{\rho \cdot V^2}{2} \cdot A$$

Where L denotes lift

c_l denotes the lift coefficient

ρ denotes fluid density

V denotes velocity

A denotes wing area

In other words, lift experienced by an airfoil is proportional to the fluid density, wing area, and velocity squared.
There are other complex dependencies represented by the lift coefficient, which will be explained below.

Coanda effect

The shape of the airfoil influences the airflow around the airfoil. The Coanda effect can be used to explain this. Both the upper and lower surfaces of the wing act to deflect air. The upper surface of the wing deflects air downwards because the airflow sticks to the wing surface and follows the tilted wing down (Merriam-Webster, 2021); this phenomenon is known as flow attachment. However, as mentioned above, the lower pressure above the wing would cause air under the wing to flow upwards, disrupting the flow attachment. This is counteracted by circulation theory.

Circulation theory

Circulation theory states that air circulates from the top to the bottom of the wing, allows pressure difference between the airfoil and contributes to flow attachment. This clockwise circulation counteracts the anticlockwise upward flow of air, allowing for flow linearity, and flow attachment, resulting in the increase of velocity of air above the wing and decreases the velocity of air below the wing. (Gilbert, 2005)

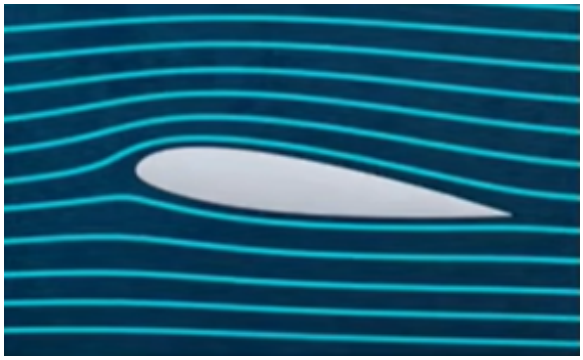

Fig 5.3a: Flow with circulation

Fig 5.3b: Flow without circulation

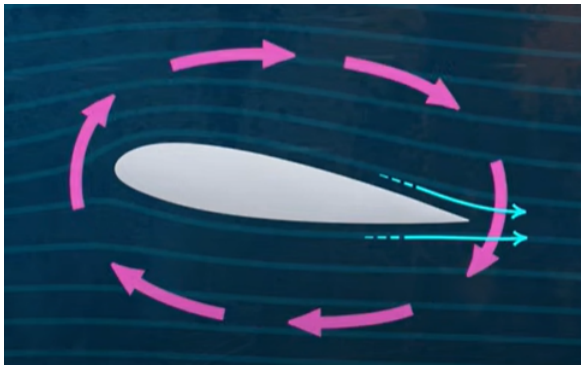

Fig 5.3c: Illustration of flow

Due to circulation theory, air flowing over the top of the wing has a higher velocity relative to the air below the wing. This results in a pressure difference, where increased pressure above the wing and lowered pressure below the wing contributes to lift.

Due to how the airfoil stays at a constant elevation, we can then neglect the fluid pressure due to gravity.

$$P_1 + \frac{1}{2}\rho v_1^{\,2} = P_1 + \frac{1}{2}\rho v_1^{\,2}$$

In other words, Static pressure above airfoil + Fluid kinetic energy per unit volume is the same above and under the airfoil.

Thus when the fluid kinetic energy per unit volume increases above the wing, the pressure decreases proportionally.

Similarly when the fluid kinetic energy per unit volume decreases under the wing, the pressure increases proportionally.

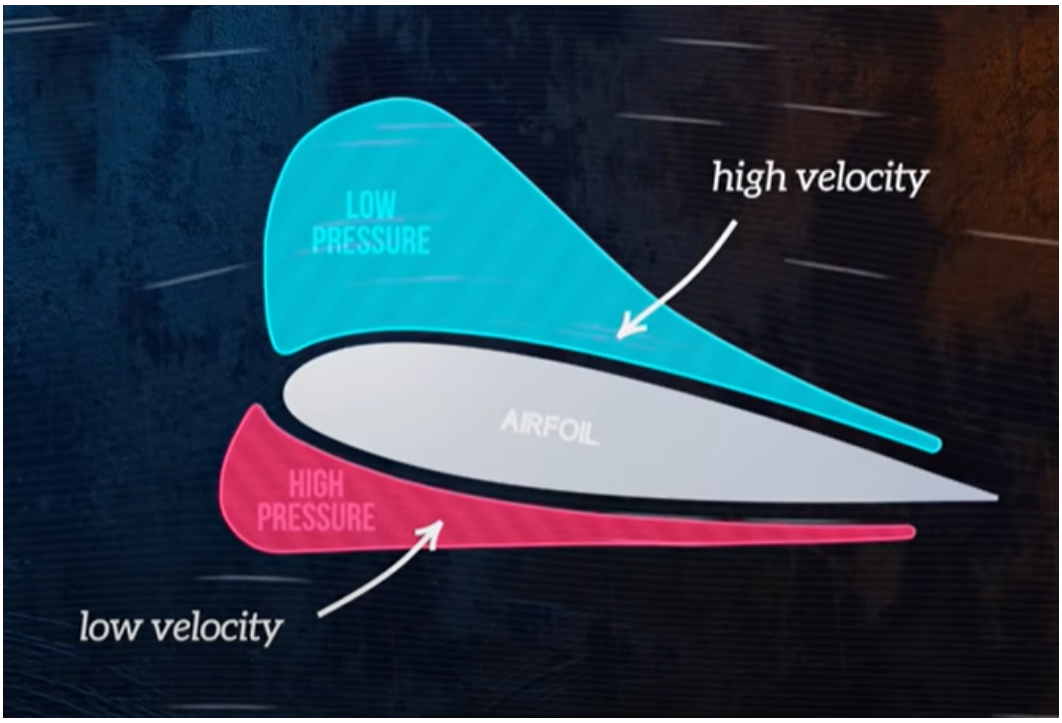

Fig 5.4: Pressure gradients of an airfoil

Newton’s third law of motion

The large volume of air displaced downwards by the airfoil through flow attachment is caused by a resultant downward force, created by flow attachment and circulation. Since the airfoil is exerting a downward force on the volume of air, according to Newton's third law, an equal and opposite force, lift, must be acting on the airfoil.

Wingtip vortices

Wingtip vortices are circular patterns of rotating air left behind a wing as it generates lift. This is caused by the pressure differences between the wings. Fluids travel from a region of higher pressure to a region of lower pressure, in this case, from under the wing to above the wing. The lack of circulation of air at the side of the wings causes the air to flow upwards from under to above the wing. When this happens, it forms a trail of air currents at the tip of the wing. (Green, 1995)

When air flows in such a way, it opposes the airflow required to generate lift, and reduces the pressure difference between the wing. The tips of the wings are thus a liability due to their inability to generate lift, while contributing to the weight of the aircraft.

Ellipse wing design

In order for the minimisation of wingtip vortices, we have adopted a design capable of preserving flow linearity through separating air of

differing pressures, therefore reducing the formation of vortices, improving upon the energy efficiency by reducing induced drag.

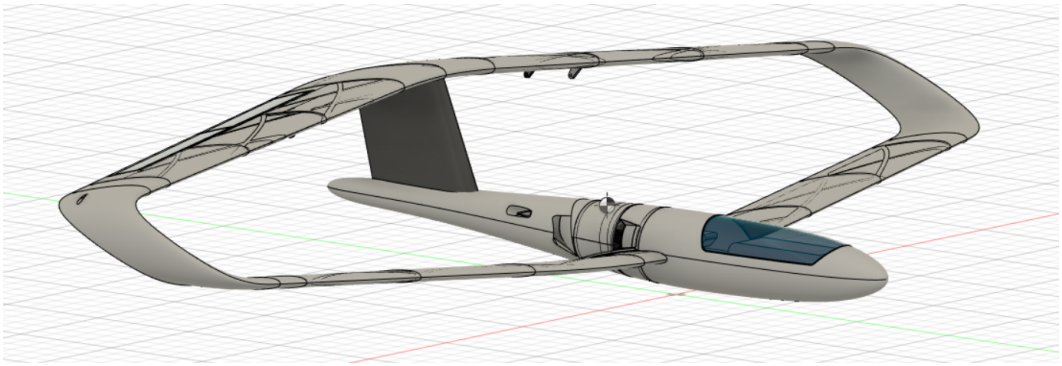

Fig 5.5: Ellipse wing design

The concept behind Avis' elliptical wing design is the usage of a connecting structure between the top and bottom wings that aids the reduction of wingtip vortices, through preventing airflow between the top and bottom surfaces of the wing.

The vertical structure connecting the wings acts as a surface for pressure dissipation, in which high pressure air traces the surface as it returns to atmospheric pressure, therefore reducing the pressure difference causing wingtip vortices.

Propulsion system

Intake amplifier design

The intake system uses another application of Bernoulli's principle, fluid entrainment.

Fluid entrainment is the transport of fluid across an interface between two bodies of fluid by a shear-induced turbulent flux. Shear force refers to a force acting in a direction that's parallel to and over the top of a surface or cross section of a body. This force is due to friction between the layers of fluids as they travel toward a certain direction, therefore pulling along other layers of fluid along with it.

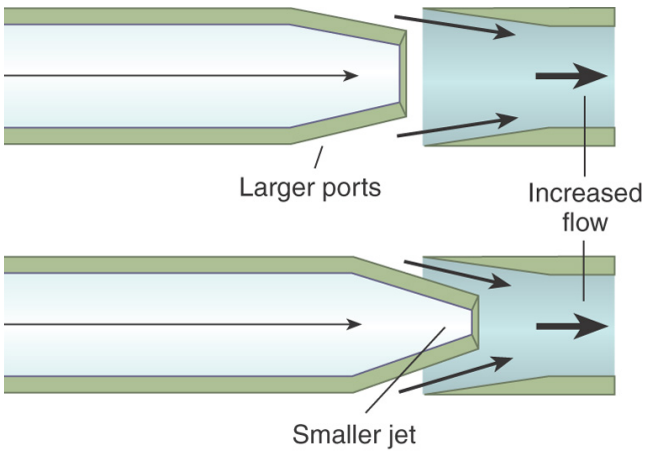

Fig 5.6: Fluid entrainment in the supplement of oxygen in oxygen masks

Using this, we can create a structure that brings in additional air through shear force, ultimately creating a drop in pressure caused by increased velocity of the air from the central tube to entrain additional air through the open port, therefore increasing the volume of air to be used as thrust.

The intake utilises the concept of fluid entrainment, in which the propeller accelerates fluid through a central tube into a second intake chamber, where shear force from the fluid in the central tube entrains additional layers of air into the thrust multiplier.

Fluid thrust multiplier design

The concept behind Avis' propulsion system is the usage of a static structure that aids the preservation of linear flow, whilst amplifying the velocity and volume of air to increase thrust. The engine structure comprises two main components, first being the intake amplifier and second being the fluid thrust multiplier. The main principle behind its design, Bernoulli's principle of fluid pressure and velocity.

Application of Bernoulli's principle

Due to how *Avis*' propulsion system does not include an increase in elevation, we can then neglect the fluid pressure due to gravity.

$$P_1 + \frac{1}{2}\rho v_1^{\,2} = P_1 + \frac{1}{2}\rho v_1^{\,2}$$

The conservation of mass, which is the principle that the mass of an object or collection of objects never changes, no matter how the constituent parts rearrange themselves, is used to present our concept design.

The conservation of mass is stated as such:

$$A_1 V_1 = A_2 V_2$$

where A is cross sectional area

V is fluid velocity

Therefore by substituting $V_2 = \frac{A_1}{A_2} V_1$

$$P_1 - P_2 = \frac{\rho}{2}(V_1^2)(\frac{A_1^2}{A_2^2} - 1)$$

Through substitution, we realise that in a horizontal flow, decrease in pressure due to an increase in cross-sectional area must result in an increase in fluid velocity, in which thrust is generated.

The Coanda effect

The Coanda effect refers to the tendency of a jet of fluid emerging from an orifice to trace an adjacent flat or curved surface. This is due to the low pressure developed between the surface and fluid, thus inducing a pressure difference. Hence, this gives way to a pressure difference in which a higher pressure above the fluid layer guides the fluid flow along the surface.

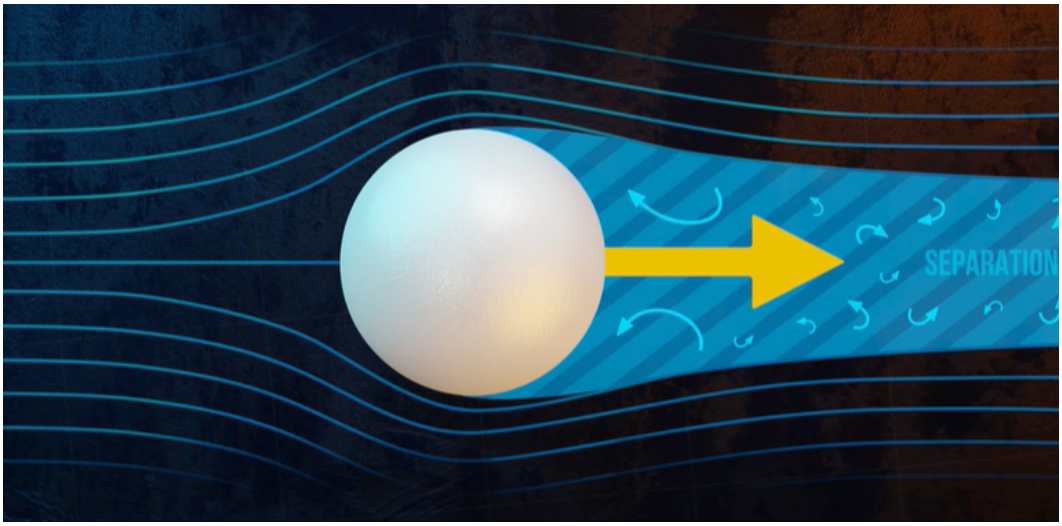

Fig 5.8: Visualisation of coanda effect

Using Bernoulli's pressure velocity concepts and the coanda effect, the thrust multiplier takes the form of an elliptical structure with an increasing cross-sectional area toward the back, along with a slit at the front end of the structure to introduce high velocity fluid.

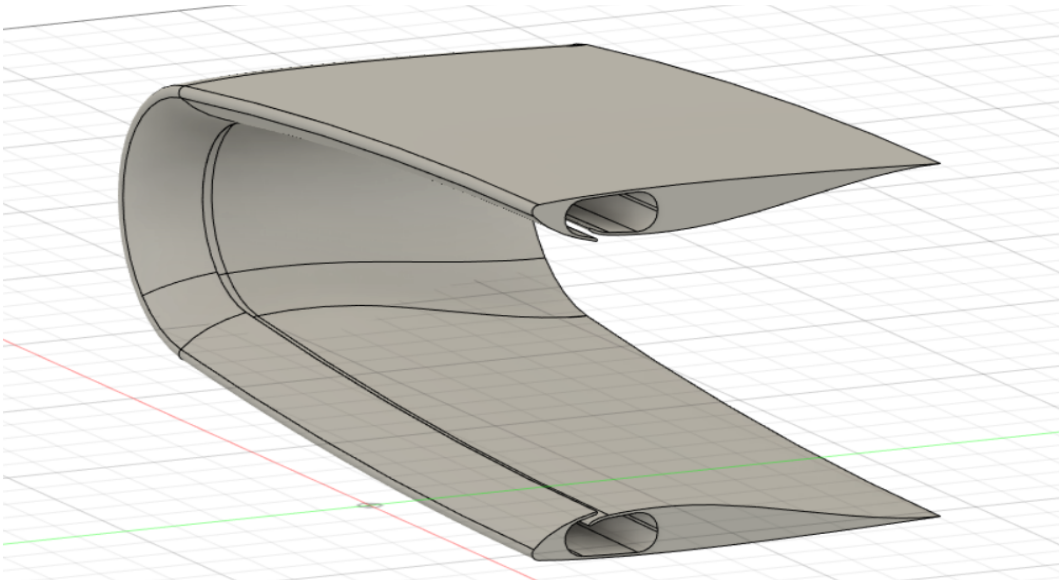

Fig 5.9: Thrust multiplier

The process in which thrust is multiplied involves two stages :

Stage 1

Air traces the inner surface of the structure as it is directed at a tangent to the surface, creating a region of low pressure near the tail of the structure as the fluid diverges, therefore decreasing air density as the same volume of air is spread out over a wider cross-sectional area.

Stage 2

The region of low pressure near the tail of the structure creates a semi-vacuum that pulls in additional air, accelerating the fluid as it travels toward the region of lower fluid. This introduces a higher volume of accelerated air into the system, therefore increasing the thrust force of Avis.

Component weight

Power 25 Brushless Outrunner Motor, 1000Kv: 3mm Bullet	- 191g
E-flite 14.8V 3200mAh 4S 30C LiPo Battery: EFLB32004S3	- 365.7g
4 Tower Pro Micro Servo SG 90	- 36g
PLA 3D-print	- 794.6g
30-Amp Pro Switch-Mode Coated BEC Brushless ESC V2: EC3	- 27.2g
Miscellaneous (sensors, port controllers)	- 189.7g
Total	- 1604.2g

Software

Data processing

Kalman filter

Kalman filtering, also known as linear quadratic estimation (LQE), is an algorithm that uses a series of measurements observed over time, including statistical noise and other inaccuracies, and produces estimates of unknown variables that tend to be more accurate than those based on a single measurement alone, by estimating a joint probability distribution over the variables for each timeframe.

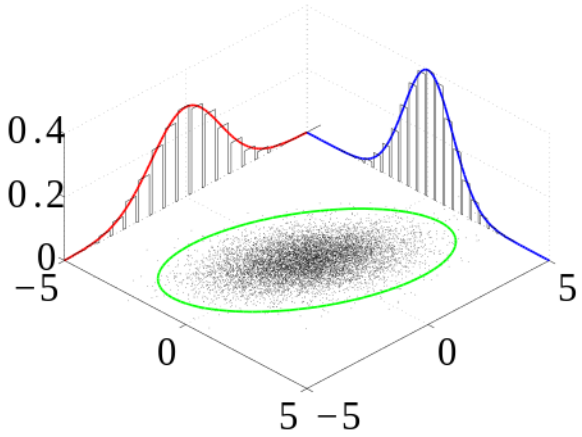

Fig 6.1: Kalman filter of 2 variables (red and blue)

The usage of Kalman filters fuses estimated values derived from multiple sensors to achieve an optimised estimate accurate to real world values.

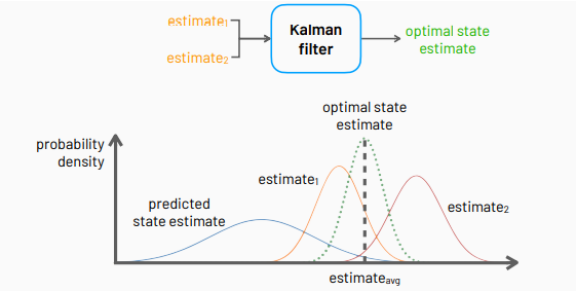

Fig 6.2: Illustration of probability distributions in a Kalman filter

In our case, the Kalman filter is applied in the determination of flight altitude.

Altitude

For the calculation of altitude, we use

$$h = \frac{P}{\rho g}$$

Where h denotes height

P denotes the pressure exerted below Avis

ρ denotes fluid density

g denotes gravitational acceleration

Mounted pressure sensors on the bottom of flatfish derives the pressure exerted on Avis, therefore allowing us to calculate the altitude. However, depending on pressure alone is insufficient as external variables like speed or wake turbulence can affect the values derived from the pressure sensor. Hence, we can use the integration of vertical velocity to determine the altitude of Avis.

To calculate vertical velocity, a inertial sensor derives the angle of flight on three axes while finding distance covered over time, therefore :

$(V_1)\ sin\ (\theta)$

Where V_1 is the plane velocity

θ is the angle from the horizontal plane

Gives us the vertical velocity, hence the vertical displacement.

By merging both values of altitude from pressure and velocity, we can then arrive at a more accurate estimate of flight altitude.

PID controller

A proportional–integral–derivative controller (PID controller or three-term controller) is a control loop mechanism employing feedback that is widely used in industrial control systems and a variety of other applications requiring continuously modulated control. A PID controller continuously calculates an *error value* $e(t)$ as the difference between a desired setpoint (SP) and a measured process variable (PV) and applies a correction based on proportional, integral, and derivative terms.

As Avis encounters uneven turbulence or cargo, it uses the PID controller to correct its flight path.

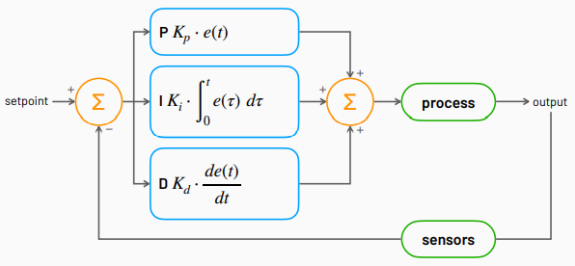

Fig 6.3: Illustration of a PID controller

A PID loop consists of 3 main components :

Proportional

The difference between the error e(t) and the setpoint objective, SP, then multiplied by a constant K_p

Integral

The sum of the instantaneous error over time and gives the accumulated offset that should have been corrected previously, then multiplied by the integral gain K_i

Derivative

The derivative of the process error is calculated by determining the slope of the error over time and multiplying this rate of change by the derivative gain K_d

By tuning the parameters K_p , K_i and K_d in response to the error e(t), the controller can precisely determine the control term to minimise error and reach the setpoint, or objective.

In our case, the setpoint is the desired velocity or altitude, the process being the varying speeds of the propeller and angle of the plane ailerons, and the errors calculated from measurements of altitude and velocity using the Kalman filter.

Methodology

The design methodology can be split into a few sections - namely mechanical design, manufacturing, software design, and analysis.

Mechanical design

The mechanical complexity of Avis requires computer-aided design software like Fusion360. This software was chosen because of its versatility and ease of use, as well as being widely accepted in the industry. Using CAD allows for a greater range of customizability in designing custom parts for the prototype. Furthermore, using such software allows the design to go through multiple iterations and overhauls easily, without any physical wastage of material.

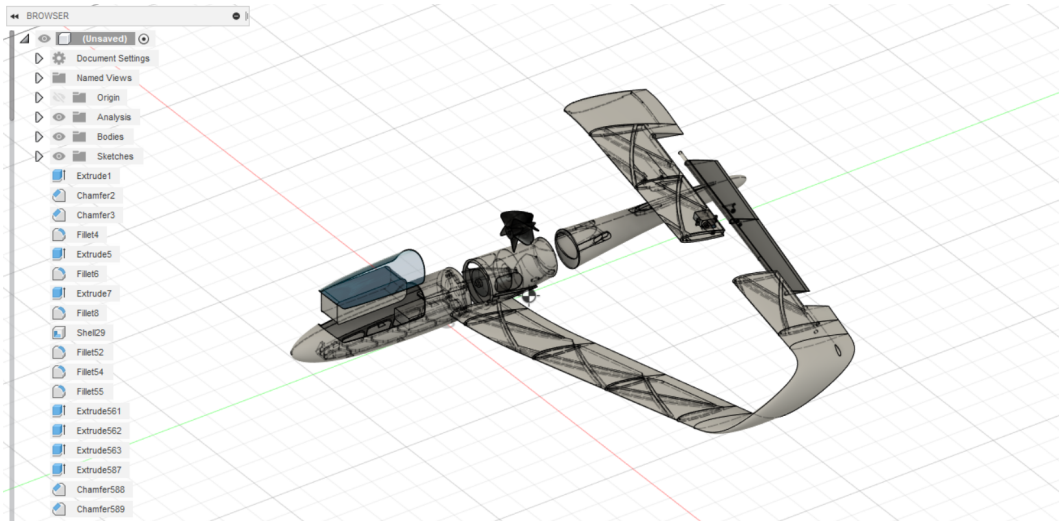

Fig 7.1: Early design stage of Avis

Fabrication

The manufacturing process of choice is 3D-printing, due to the ease of use and versatility of such a fabrication method. The autonomous and low cost 3D-print process is a valid choice for prototyping due to its precision and efficiency in replicating organic designs.

Fig 7.2: 3D-print process

Completed models are then sliced in Ultimaker Cura v4.0, a software designed for optimising the 3D printing process. With over 400 settings for print speed, temperature, structural supports, detail, etc; Cura provides detailed calibration for our manufacturing process, creating a product accurate to the 3D model.

Furthermore, our design process considers the layer-by-layer process of 3D-printers, decreasing additional material used for supports while minimising chances for warps due to overarching structures.

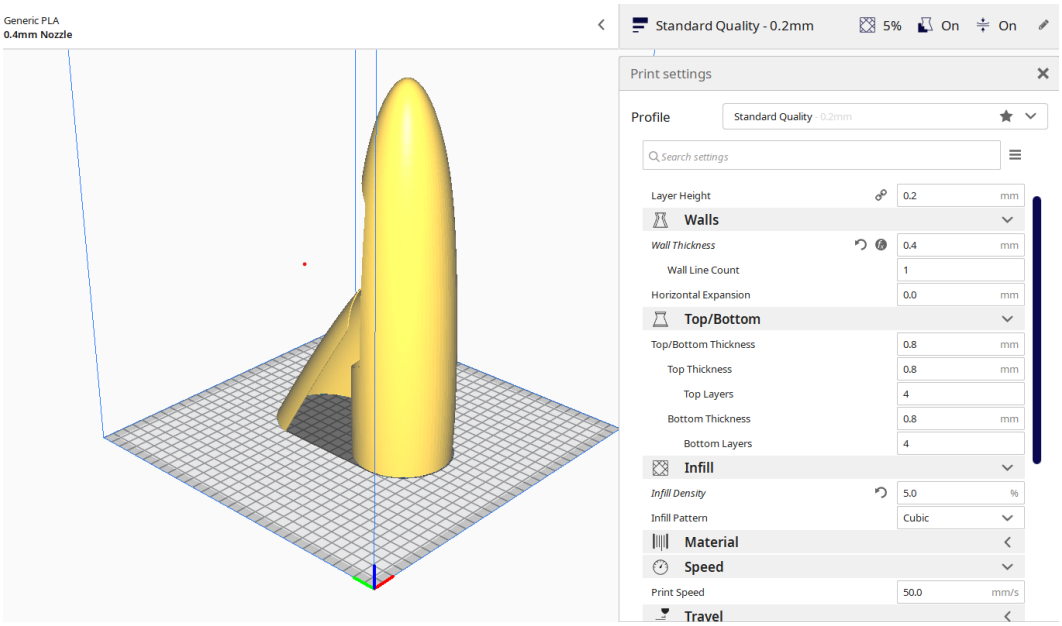

Fig 7.3: Ultimaker Cura

For printing the plane, polylactic acid (PLA) was used. PLA is the most widely used filament in 3D printing. (Alsop, 2018) PLA has many benefits, as it is cheap, relatively light, and easy to use. PLA has a density of 1.21 - 1.43gcm^{-3} (Matbase, 2012), which is relatively lightweight, making it a suitable material for the plane. PLA is relatively cheap compared to other variants like nylon (UMass, 2021), which helps us drive down the total cost of the plane.

Analysis

Most components of the plane have undergone rigorous vetting and evaluation for design optimisation. Platforms like Fusion and Autodesk CFD provide simulation workspaces that test and analyse components

under set parameters, providing the ability to tweak our designs without any wastage of materials.

Computational fluid dynamics

Autodesk CFD was used to measure the aerodynamic properties of *Avis*. This allowed us to accurately identify the parts of the plane that were causing drag, and thus rectify the issue quickly.

k - ε turbulence model

The K-epsilon (k-ε) turbulence model is the most common model used in computational fluid dynamics (CFD) to simulate mean flow characteristics for turbulent flow conditions. It is a two equation model that gives a general description of turbulence by means of two transport equations.

For turbulent kinetic energy k

$$\frac{\partial}{\partial t}(\rho k) + \frac{\partial}{\partial x_i}(\rho k u_i) = \frac{\partial}{\partial x_j}\left[\left(\mu + \frac{\mu_t}{\sigma_k}\right)\frac{\partial k}{\partial x_j}\right] + P_k + P_b - \rho\epsilon - Y_M + S_k$$

For dissipation ϵ

$$\frac{\partial}{\partial t}(\rho\epsilon) + \frac{\partial}{\partial x_i}(\rho\epsilon u_i) = \frac{\partial}{\partial x_j}\left[\left(\mu + \frac{\mu_t}{\sigma_\epsilon}\right)\frac{\partial \epsilon}{\partial x_j}\right] + C_{1\epsilon}\frac{\epsilon}{k}\left(P_k + C_{3\epsilon}P_b\right) - C_{2\epsilon}\rho\frac{\epsilon^2}{k} + S_\epsilon$$

*Fig 7.4: Illustration of k-**ε** model*

Or simply,

Rate of change of k in time + **Transport of k** by advection = **Transport of k** by diffusion + Rate of production of k - Rate of **destruction of k**

Rate of change of ε in time + **Transport of ε** by advection = **Transport of ε** by diffusion + Rate of production of ε - Rate of **destruction of ε**

Where

μ_i $is\ the\ velocity\ component\ in\ the\ specified\ direction,$

E_{ij} $is\ the\ rate\ of\ deformation,$

μ_t $is\ eddy\ viscosity$

The other variables are model constants that were derived through data fitting using data from a range of turbulent flows.

They are,

C_{1e}, $coefficient\ of\ 1e\ =\ 1.44$

C_{2e}, $coefficient\ of\ 2e\ =\ 1.92$

σ_k, $standard\ deviation\ of\ k\ =\ 1.0$

σ_ϵ, $standard\ deviation\ of\ \varepsilon\ =\ 1.3$

The model uses calculations involving **free shear flows**, small pressure gradients, and confined flows. This is useful in calculating the fluid dynamics of Avis due to it being in a free shear flow.

The model is also most commonly used in scenarios where only the initial conditions and boundary conditions need to be supplied for calculations.
During calculations,
Our initial conditions being the velocity of approaching air, and the density of approaching air
Our boundary conditions being set to the area around Avis

With this we were able to obtain the shear forces, and by an extension the forces acting on Avis through relating the produced energies within each region using the Kinetic-epsilon model.

Drag coefficient

For each individual CFD model, the drag coefficient was calculated to accurately determine the amount of drag force created.

The drag coefficient is a dimensionless quantity, which is used to quantify the drag or resistance of an object in a fluid environment, such as air. The drag coefficient is thus proportional to the aerodynamic properties of an object - a lower drag coefficient indicates that the object is more aerodynamic. The drag coefficient is defined:

$$C_d = \frac{2F_d}{\rho u^2 A}$$

where C_d is the drag coefficient;

F_d is the drag force;
ρ is the fluid density;
u is the flow speed of the object; and
A is the reference area.

The total drag force is calculated in the simulation. Afterward, known values can be substituted into the equation to find C_d.

Procedure

To prepare the model for simulation, small features that would complicate the simulation - such as small chamfers and cavities - were

removed from the model. This helps to reduce the complexity of the simulation without greatly affecting the end results.

Static stress analysis

The wings of the plane places stress on the body, to prevent the wings from collapsing. To ensure the structural integrity of the design, Fusion 360 was used to simulate the static stress on the plane. Thus, areas under greater stress can be accurately identified, and given extra support, whereas areas under lower load can have unnecessary support removed, to help save material and production time, while also making the design simpler.

Results

Static stress analysis

Wing integrity

Several design optimisations were made with the aid of the simulation platform on Fusion360, being the improvement of the structural integrity of the wing.

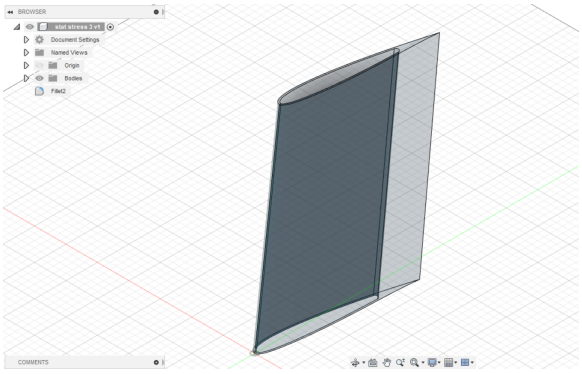

Fig 8.1a: Initial wing design

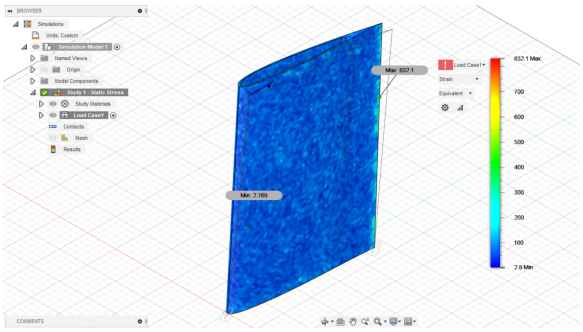

Fig 8.1b: Strain graph of initial design

Upon application of a 10N force on the leading edge of the wing component, the initial design has a minimum stress of 3392 Mpa with a maximum stress of 1631000 Mpa.

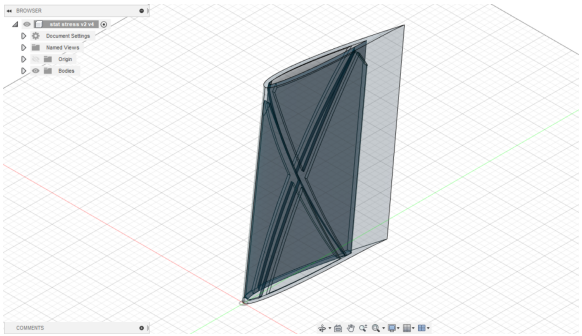

Fig 8.2a: Adapted wing design

Improvement upon the wing design includes the crossbeam structures. The intention of these crossbeams is for the redistribution of pressure from a single point to the rest of the wing body, as well as additional structural integrity through uni-directional support.

The addition of such structures absorbs additional force acting on the wing, distributing stress on the wing to said structures to decrease overall static stress per unit volume.

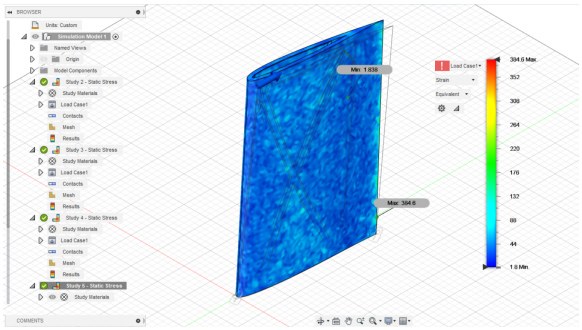

Fig 8.2b: Stress analysis of redesigned wing component

As shown in figure 8.2b, the minimum stress has been decreased to 1850 Mpa while maximum stress has been decreased to 768389 Mpa, a 55% reduction in the chance of deformation, proving the utility of cross beams in improving structural stability.

Computational fluid dynamics

Assumptions

Simulations were performed for Avis to prove the following concepts. From the ***k - ε turbulence model,*** we established the need for boundary conditions.

Since physical testing could not be carried out, we were unable to obtain accurate boundary conditions. We thus assumed the boundary conditions to be the minimum required values for flight.

Assumptions are as such:

Terminal velocity of Avis: 6m/s

When V = 6m/s, we can achieve the required lift, L = 16N (being the weight of Avis) to enable flight.

L was determined using simulations(more below) under assumptions of terminal velocity.

Determination of lift

Lift can be represented as such:

$$L = c_l \cdot \frac{\rho \cdot V^2}{2} \cdot A$$

Where L denotes lift

c_l denotes the lift coefficient

ρ denotes fluid density

V denotes velocity

A denotes wing area

Simulations show that at an air velocity of m/s, lift generated by the ellipse wing, L = 16N (being the weight of Avis).

Determination of drag and thrust

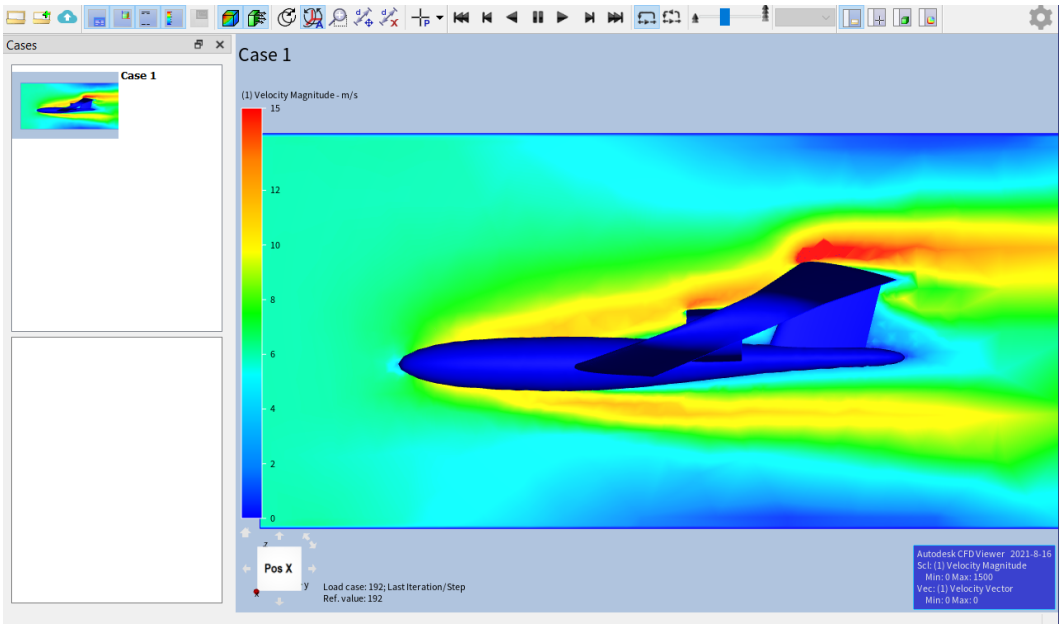

Fig 8.3: Velocity graph showing airflow around Avis

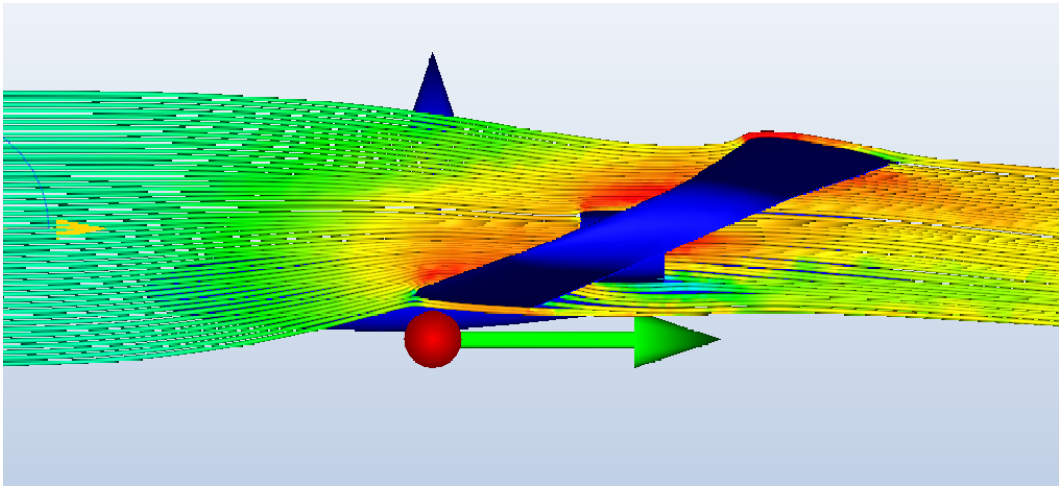

Fig 8.4: Traces showing airflow around Avis

Simulations show that drag generated by Avis at 6m/s, D = 4.98N

Thus to achieve required terminal velocity, thrust generated by Avis at 6m/s, F = 4.98N

To achieve F = 4.98N , we can use this equation to determine P_2:

$$F = A\Delta P$$

Where F is the thrust

A is the propeller area

ΔP is the difference in pressure across propeller

$$4.98N = 0.0025m^2(P_1 - P_2)$$

P_2 = 103317

ΔP = 1992 Pa

Thus:

Input air pressure of propeller, P_1 = 101325 Pa (1atm)

Output air pressure of propeller, P_2 = 103317 Pa

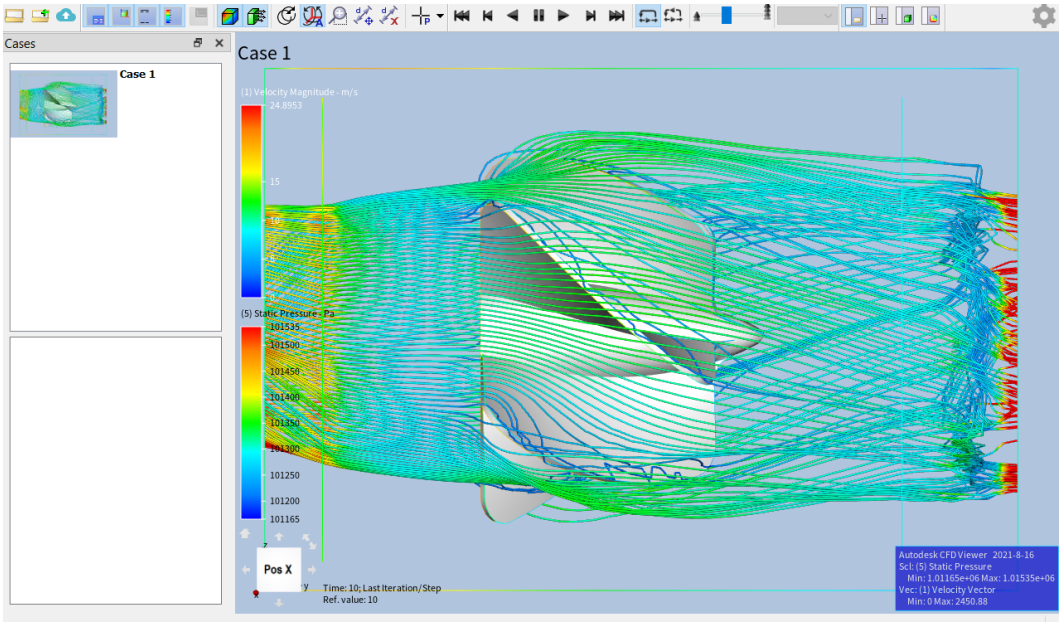

Fig 8.5: Traces around propeller

With the values found above, we were able to simulate the airflow of our propeller.

Drag reduction

In order to justify the streamlined shape of Avis, a comparison study was made on two different objects, a near flat plane and a teardrop structure

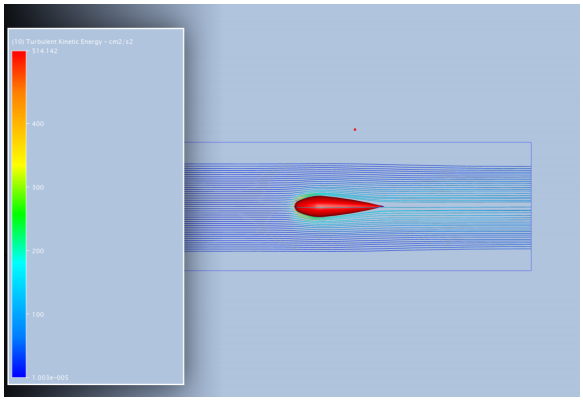

Energy flow trace of teardrop

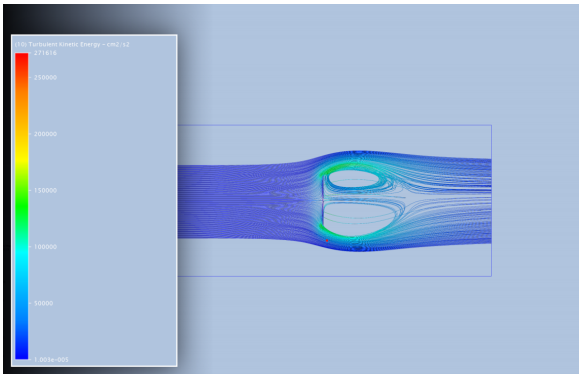

Energy flow trace of flat plane

Observing the two different structures, we can see the appearance of eddies, or swirling fluids. These eddies are caused by the low pressure brought behind the model, therefore separating flow into a turbulent, swirling fluid. These vortices are a form of induced drag as they siphon useful energy input into the system for parasitic forces that do not act in favour of thrust.

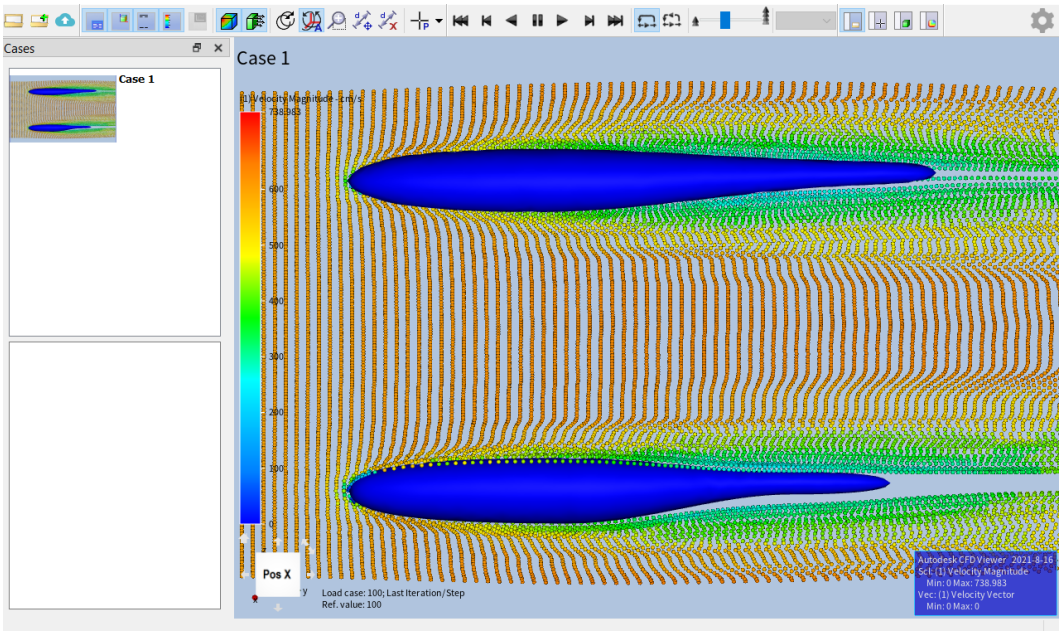

Fig 8.6: Traces around body

Applying the above concept of parasitic drag in relation to flow separation, we observe the earlier model (bottom) with a higher flow separation as compared to the later model (top) in which particles eventually form a linear flow trailing the edge. Hence, optimisation of the body by decreasing the changes in angle in relation to the body surface reduces flow separation, hence reducing parasitic drag.

Propulsion system

Results computed from computer aided simulations prove to be supportive of the thrust multiplication concept, demonstrating a drastic decrease in fluid pressure followed by an increase in thrust.

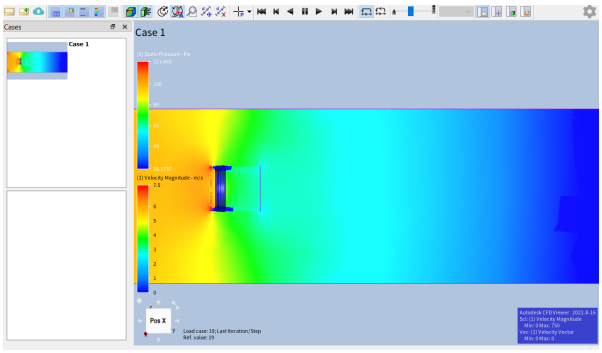

Fig 8.7: Pressure graph

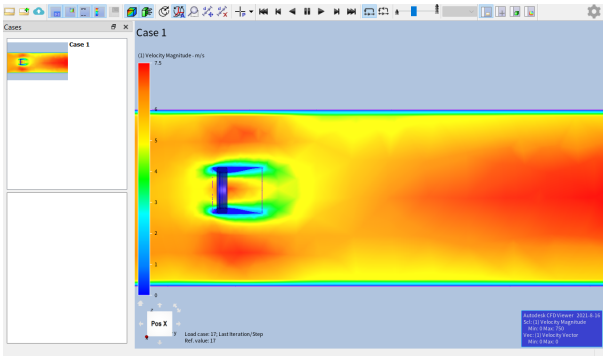

Fig 8.8: Velocity graph

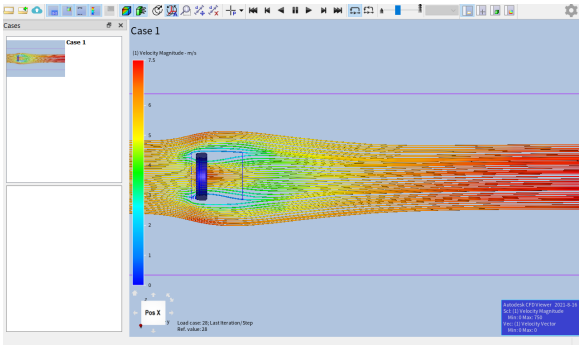

Fig 8.10: Traces showing airflow behind engine

As shown in fig 8.7, the pressure in the engine is lower compared to the atmospheric pressure, inducing air into the structure at high speeds, increasing the output volume of air through the thruster.

As shown in fig 8.8, the air speed within the engine is increased to 7.3m/s, causing an increase in volume of air thrusted through the structure, therefore contributing to thrust.

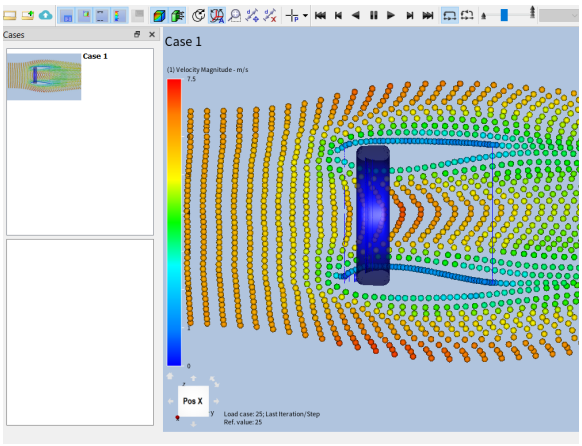

Fig 8.9: Traces showing airflow inside engine

Conclusion

This study has shown two main benefits that originate from the preservation of linear flow, being the reduction of vortices and the minimisation of induced drag.

Limitations

The restriction upon possible materials like lightweight PLA has increased the density of the plane by a large margin due to the ongoing pandemic.

Furthermore, COVID-19 has restricted the experimental data gained as facilities from higher institutes were inaccessible.

Future work

Improvement upon air input through highly efficient systems like combustion chambers to fully utilise the air multiplication components of the propulsion system.

Further testing upon airfoil geometry to maximise lift of the aircraft, requiring further physical experimentation

References

Aboulafia, Richard; Michael, Kevin(16 July, 2018). "The Global Aerospace Industry Size & Country Rankings". The Teal Group / AeroDynamic Advisory. https://aerodynamicadvisory.com/wp-content/uploads/2018/07/AeroDynamic-Teal_Global-Aerospace-Industry_16July2018.pdf

Alsop, Thomas. (2018) “Worldwide most used 3D printing materials, as of July 2018”. Statistica. https://www.statista.com/statistics/800454/worldwide-most-used-3d-printing-materials/

Autodesk. (2018). “Calculating the Coefficient of Drag - Urbee Example”. https://knowledge.autodesk.com/support/cfd/learn-explore/caas/simplecontent/content/calculating-the-coefcient-drag-urbeeexample.html

Autodesk. (2020). “Manual Mesh Sizing”. https:// knowledge.autodesk.com/support/cfd/learn-explore/caas/CloudHelp/cloudhelp/2019/ENU/SimCFD-UsersGuide/files/GUIDDC8D7EDA-5E18-4088-93AB-3BB517D6469C-htm.html

Autodesk. (2020). “Turbulence”. https://knowledge.autodesk.com/support/cfd/learn-explore/caas/CloudHelp/cloudhelp/2019/ENU/SimCFD-UsersGuide/files/GUIDE9E8ACA1-8D49-4A49-8A35-52DB1A2C3E5F-htm.html

Batchelor, G. K. (1967) “Introduction to Fluid Dynamics.” Cambridge University Press.

156-164

https://books.google.com.sg/books?id=Rla7OihRvUgC&pg=PA156

Engineering clicks. (2021). Understanding lift

https://www.engineeringclicks.com/lift-equation/

Federal Aviation Administration (10 February, 2014). “Advisory Circular on Aircraft Wake Turbulence.”

https://www.faa.gov/documentLibrary/media/Advisory_Circular/AC_90-23G.pdf

Gilbert, Lester. (18 December, 2005) “Circulation Theory of Lift”.

http://www.onemetre.net/design/downwash/Circul/Circul.htm

Green, Sheldon. (1995) “Wing Tip Vortices”. Kluwer Academic Publishers.

https://books.google.com.sg/books?id=j6qE7YAwwCoC&pg=PA427

Material Properties Database. (2012) “Material Properties of Polylactic Acid (PLA), Agro Based Polymers".

http://www.matbase.com/material/polymers/agrobased/polylactic-acid-pla/properties

Merriam-Webster. (2021) “Coanda effect”.

https://www.merriam-webster.com/dictionary/Coanda%20effect

MIT Department of Aeronautics and Astronautics. (16 March 1997). “Theory of Flight”.

https://web.mit.edu/16.00/www/aec/flight.html

Ranter, Harro (November 12, 2001). "ASN Aircraft accident Airbus A300B4-605R N14053 Belle Harbor, NY". Aviation Safety Network.

http://aviation-safety.net/database/record.php?id=20011112-0

Skybrary (2020). “Induced Drag”.

https://www.skybrary.aero/index.php/Induced_Drag

Teach engineering. (2021)

https://www.teachengineering.org/lessons/view/cub_bernoulli_lesson01

The Efficient Engineer. (6 October 2020). “Understanding Bernoulli’s Principle”.

https://www.youtube.com/watch?v=DW4rItB20h4&t=34s

Theory of flight

https://soaneemrana.org/onewebmedia/THEORY%20OF%20FLIGHT.Pdf

University of Massachusetts Amherst. (2021) “Materials and Pricing”

https://www.library.umass.edu/dml/3dprinting/materials/